Transient oscillations in the vicinity of excitons and in the band of semiconductors

J. P. Sokoloff
Optical Sciences Center, University of Arizona, Tucson, Arizona 85721

M. Joffre
Laboratoire d'Optique Appliquée, Ecole Polytechnique–Ecole National Supérieure de Techniques Avancées (ENSTA), 91120 Palaiseau, France

B. Fluegel
Optical Sciences Center, University of Arizona, Tucson, Arizona 85721

D. Hulin
Laboratoire d'Optique Appliquée, Ecole Polytechnique–Ecole National Supérieure de Techniques Avancées (ENSTA), 91120 Palaiseau, France

M. Lindberg and S. W. Koch
Optical Sciences Center and Physics Department, University of Arizona, Tucson, Arizona 85721

A. Migus and A. Antonetti
Laboratoire d'Optique Appliquée, Ecole Polytechnique–Ecole National Supérieure de Techniques Avancées (ENSTA), 91120 Palaiseau, France

N. Peyghambarian
Optical Sciences Center, University of Arizona, Tucson, Arizona 85721
(Received 29 February 1988; revised manuscript received 10 May 1988)

Several semiconductor materials, including CdS, CdSe, GaAs, and GaAs-$Al_xGa_{1-x}As$ multiple quantum wells were studied with use of femtosecond pump-probe spectroscopy. Oscillatory structures are observed in the differential transmission spectra of the probe pulse at the very early times when the probe pulse precedes the pump pulse. In addition to oscillations around the exciton frequency when pumping is either above or below the exciton, oscillatory structures are also observed in the vicinity of the pump frequency when the pump is tuned inside the semiconductor band. A semiclassical theory qualitatively explains the observed data. These oscillations are found to be the precursors of spectral hole burning (oscillations around the pump for pumping into the band), exciton bleaching (oscillations around exciton for pumping into the band) and exciton optical Stark shift (oscillations around exciton for pumping below the band).

I. INTRODUCTION

The dynamics of a semiconductor shortly after optical excitation has been studied extensively in the last decade.[1–15] The development of picosecond-laser systems first made possible the direct observation of hot-carrier distributions.[1–4] Later, femtosecond systems allowed the study of such fast processes as spectral hole burning.[6,7] The processes that involve carrier excitation in the conduction band are not coherent in the strict sense of the definition that a coherent system oscillates in phase with the exciting field, because the light pulses of $\cong 100$ fs duration are either comparable to or longer that the dipole decay rate. True coherent effects associated with discrete exciton states, however, can be observed with the available pulses as the coherence decay time for excitons is long on the femtosecond time scale.[8–14]

Recently, we reported oscillatory structures in the transmission spectra of bulk GaAs and CdSe at times before the arrival of the peak of the exciting pulse.[12,13] These oscillatory features, however, are general and can be observed in any semiconductor. We highlight that fact here by presenting a comprehensive study of the temporal evolution of the oscillatory features in molecular-beam-epitaxy (MBE) -grown GaAs and GaAs-$Al_xGa_{1-x}As$ multiple quantum wells (MQW's), bulk CdS, and CdSe. Oscillations in the differential transmission spectra are reported in the region around the exciton when the pump is below or above the band edge, and in the region of the pump when the pump is above the band edge. No oscillations are seen in the region of the pump when the pump is tuned below the band edge. Our results are in qualitative agreement with the recently developed theory and we find that for pumping below the band edge, the oscillations around the exciton are the transient precursors to the optical Stark shift.[10,11] Oscillatory structures around the pump when the pump is tuned above the band edge are the transient precursors of

spectral hole burning. And, finally, oscillations around the exciton for pumping far above the band gap are the initial consequence of exciton bleaching.[13]

In this paper the experiments and the results are described in Secs. II and III, respectively. A comparison of these results with theory is given in Sec. IV. Finally, the paper is closed with a discussion in Sec. V.

II. EXPERIMENT ARRANGEMENT

Standard femtosecond time-resolved pump-probe experiments were carried out on systems in Tucson (8-kHz system) and Palaiseau (France) (10-Hz system). Both systems used a balanced colliding-pulse mode-locked laser (CPM) to generate $\cong$100-fs pulses at 620 nm. In the system used to study bulk and MBE-grown GaAs, a 10-Hz Nd-YAG (YAG denotes yttrium-aluminum-garnet) laser was used to amplify the output pulses of the CPM. Part of the amplified output was sent through a water cell to generate a broadband probe. The remainder of the 620-nm beam was the source of the pump, either at its original wavelength or around 800 nm. The 800-nm operation was accomplished by sending the amplifier output through a second water cell followed by spectral filtering and a second amplifier. GaAs MQW's, CdSe, and CdS were studied on the second system, which used an 8.5-KHz copper-vapor laser amplifier and an ethylene-glycol jet to produce the continuum probe. This system used a 620-nm pump for all experiments.

Figure 1 shows the experimental arrangement. The pump and probe were focused at a relative angle of $\cong 15°$ onto the sample, which was mounted in a cryostat. The transmission of the probe is detected as a function of wavelength at various time delays between the pump and probe pulses using a spectrometer followed by an optical multichannel analyzer. The delay between the two pulses is controlled by a stepper motor which changes the length of an optical delay line. Either the normalized differential transmission spectra (DTS) $\delta T=(T-T_0)/T_0$, or minus the differential absorption multiplied by the sample thickness (which is equal to δT for small signals) was measured in all of the experiments. Here, T_0 is the linear probe transmission and T is the probe transmission with the pump present.

III. EXPERIMENTAL RESULTS

As mentioned above, we studied coherent transients in three cases distinguishable by the pump frequency relative to the band edge and the spectral region probed. In particular, we measured the δT in the vicinity of (i) the pump when the pump is far above the band edge, (ii) the exciton when the pump is below the band edge, and (iii) the exciton when the pump is far above the band edge.

Figure 2(a) shows the results for case (i) for a $\cong$0.5-μm-thick CdSe platelet ($\lambda_{gap}\cong 670$ nm) pumped at 620 nm. At a time delay of -10 ps (the minus sign indicates that the probe precedes the pump), no transmission changes have occurred and only the background noise is present. Starting at -800 fs, oscillations appear which increase in magnitude and decrease in frequency as the time delay approaches zero. The oscillations are symmetric about the pump and are contained in an envelope which roughly follows the pump spectrum. For the curve at -100 fs the oscillations have disappeared, and the peak, which is centered at the pump wavelength, rapidly grows and broadens into a feature characteristic of state filling by a nonthermal distribution of carriers (spectral hole). Figure 3 shows similar results in a GaAs-$Al_xGa_{1-x}As$ MQW with 100-Å wells at room temperature. The spectra again contains oscillations that broaden and evolve into a central peak. The linear dependence of oscillation frequency on time delay is clearly visible. This dependence is shown in Fig. 4 where we have plotted the frequency of the oscillations (the inverse of the fringe spacing of the oscillatory structures in units of femtoseconds) of Fig. 3 versus time delay. The frequency of oscillations was measured away from the central peak to avoid any influence from the hole burning. In this curve the absolute position of zero has been changed.[16] Note that the measurement of the oscillations is a very convenient method to determine the absolute

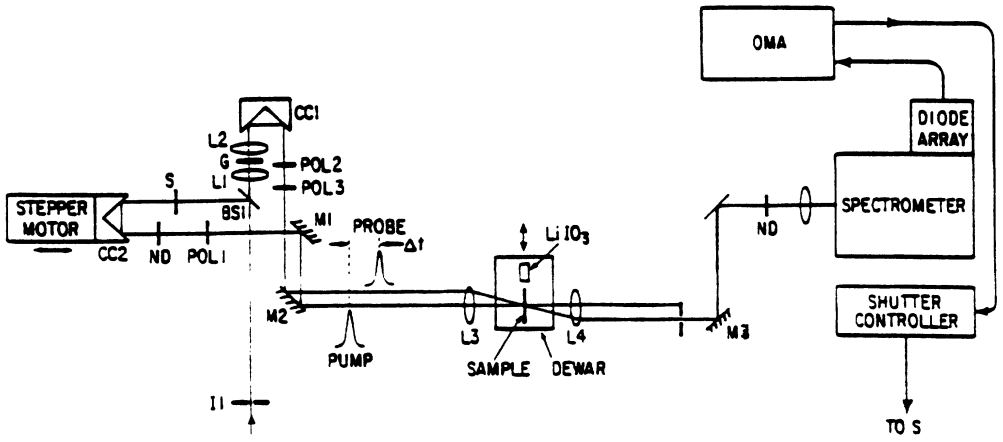

FIG. 1. Experimental arrangement for the time-resolved pump-probe experiments reported in this paper.

position of zero time delay.

The next two experimental cases involve the spectral region around the exciton. Figure 5(a) shows the results of the differential transmission measurements for a 0.5-μm-thick MBE-grown layer of bulk GaAs at 15 K when the pump was tuned just below the 818-nm exciton reso-

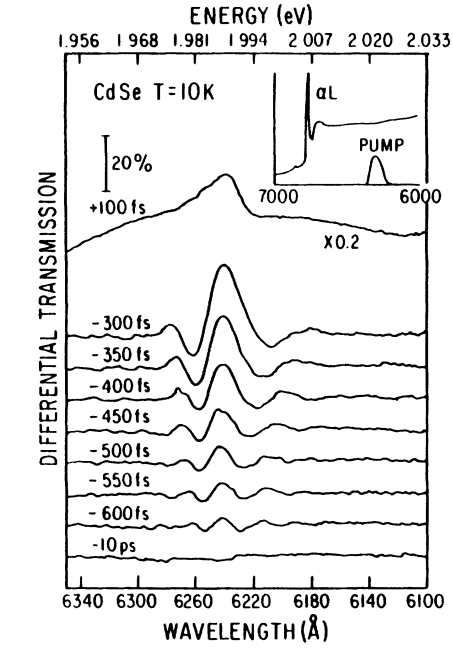

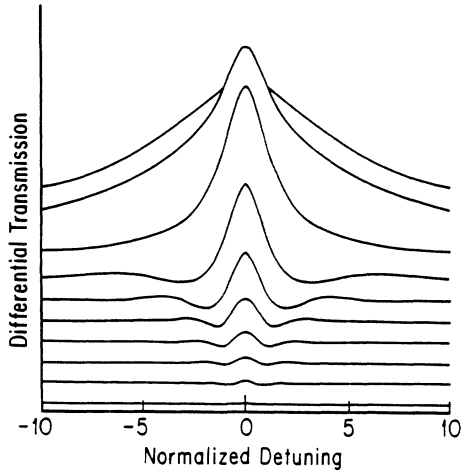

FIG. 2. (a) Measured differential transmission spectra around the pump wavelength in a 0.5-μm-thick CdSe platelet at 10 K. The pump pulse is centered around 620 nm, it has a 150-fs FWHM, and a peak intensity of 10^9 W/cm^2. Curves are taken at (lower to upper curve) -10000, -800, -750, -700, -650, -600, -550, -500, and -100 fs. The last curve is compressed by a factor of 5; (b) differential transmission spectra calculated for interband excitation. The central pump frequency Ω_L is assumed to be well above the semiconductor band gap. The detuning is normalized to $\sigma^{-1}=120/(2\ln 2)$ fs. The temporal FWHM of the pump pulse is 120 fs and the damping constants have been taken as $\gamma=0.035$ fs^{-1} and $\Gamma=1/100$ fs^{-1}. Various curves are for different time delays t_p between pump and probe. The bottom curve is for $t_p=-400$ fs and the top curve is for $t_p=50$ fs. The curves are in 50-fs intervals.

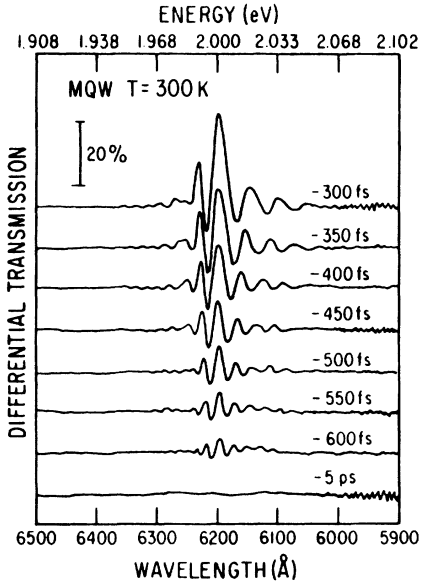

FIG. 3. Measured differential transmission spectra near pump wavelength in a 0.75-μm-thick, 100-Å GaAs-$Al_xGa_{1-x}As$ multiple quantum well at 300 K. The pump pulse is centered around 620 nm, it has a 150-fs FWHM, and a peak intensity of 10^9 W/cm^2. Delay times (in fs) are -5000, -800, -750, -700, -650, -600, -550, and -500.

nance. The curves are 200 fs apart. The inset in Fig. 5(a) displays the position of the pump relative to the exciton peak. The oscillations are now centered around the exciton with increasing amplitude as the time delay approaches zero. However, unlike the previous case, the shape of the oscillations is asymmetric, always with the largest positive peak on the side toward the pump and the largest negative peak away from the pump. The oscilla-

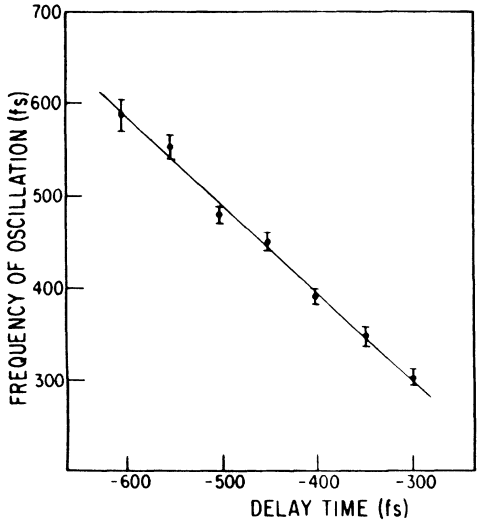

FIG. 4. Measured frequency of oscillations (Ref. 16) (inverse of the fringe spacings) for the spectra of Fig. 3 (bars). Calculated frequency of oscillations for the case shown in Fig. 2(b) as a function of time delay t_p (line).

tions later develop into a dispersive-looking feature indicative of a blue shift of the exciton resonance.

In Fig. 6 the differential transmission is shown for pumping below the exciton in a thin CdS platelet at 150 K. The DTS are similar to those in Fig. 5(a) and this supports are assertion that the observed effects are general and do not depend on the choice of samples. Again, as in Fig. 5(a), asymmetric oscillations are seen in the vicinity of the exciton resonance, which, with increasing temporal overlap between pump and probe, evolve into a dispersive-looking feature like that in Fig. 5(a).

For case (iii) we present the series of curves for 0.5-μm-thick GaAs and CdSe samples shown in Figs. 7(a) and 8. For both samples the pumping frequency is at 620 nm, which is above the band gap of both materials. In Fig. 7(a) the data for GaAs are plotted at 15 K. The curves have time delays which are 100 fs apart and, spectrally, are centered around the exciton resonance at 818.3 nm. For early delays there are symmetric oscillations around the exciton very similar to those around the pump in case (i). The amplitude of the oscillations increases with decreasing time delay between the pulses. The frequency of the oscillations is found to vary proportionally to the time delay. The evolution of the oscillations, as the time delay goes through zero, can be seen in the later curves. The oscillations gradually disappear, and the central peak assumes the spectral shape of the exciton. This is characteristic for the bleaching of the exciton resonance. Figure 8 shows the same experiment in the CdSe platelet at 10 K. The curves are taken every 50 fs and the oscillations are centered around the B exciton at 669 nm.

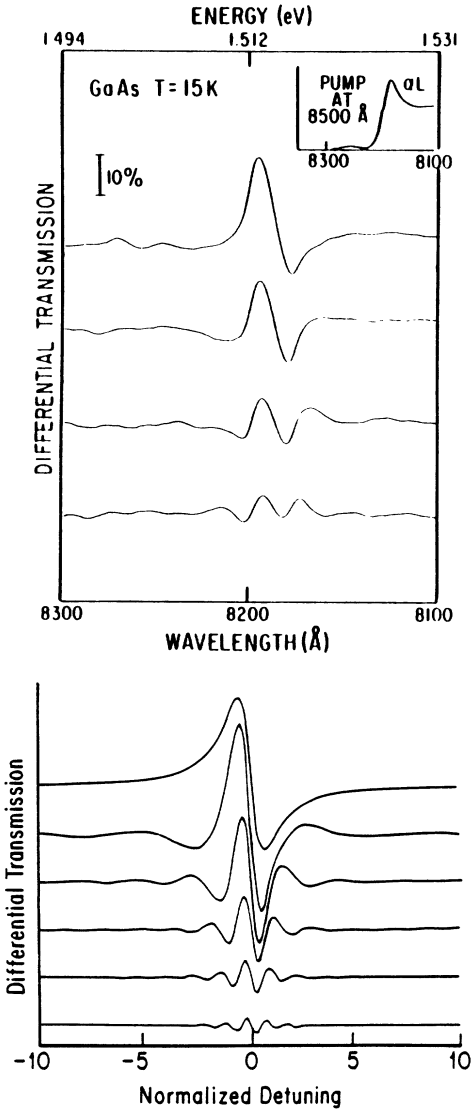

FIG. 5. (a) Measured differential transmission in the spectral region of the exciton for a 0.5-μm thick bulk GaAs sample excited below the exciton resonance. The sample temperature is 15 K and the pump pulse is centered around 850 nm with 300-fs duration. Delay times are 200 fs apart; (b) differential transmission spectra calculated in the spectral vicinity of the exciton resonance ω_x. The central pump frequency Ω_L is assumed to be detuned by -10σ and the temporal FWHM of the pump pulse is 120 fs. The curves are for different time delays t_p with 100-fs intervals, starting from the bottom at -500 fs to the top curve which is for 0 fs.

IV. COMPARISON WITH THEORY

To explain the observed experimental results, we apply a semiclassical theory (Refs. 17, 18, and the preceding paper, Ref. 19) that has been developed to calculate the changes in a weak probe transmission through a medium that are caused by the interaction between the polarization of that medium and a strong femtosecond optical excitation. The slowly varying amplitude approximation is used and the propagation effects in the sample are neglected, hence restricting the validity to optically thin samples. However, these conditions are easily met in the

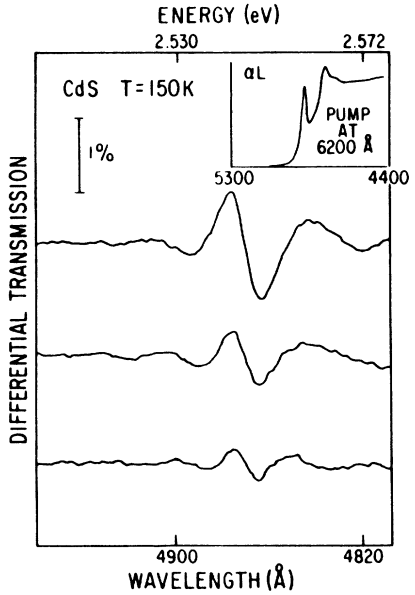

FIG. 6. Measured differential transmission spectra in the exciton region in a thin CdS platelet for below-resonance pumping. The sample temperature is 150 K and the pump pulse is centered around 620 nm. The spectra were taken in 100-fs intervals.

reported experiments which used pump pulses $\cong 100$ fs long ($\cong 50$ optical cycles) and samples of thickness $L < 0.5\,\mu$m.

In this approach the differential transmission spectra at very early times are calculated by assuming that the different dipole-coupled k states in the semiconductor bands react independently to the exciting light. The total response is obtained by computing the response of an individual k state separately and then integrating the result over all k values. In this integral the density of states is that of an electron-hole system with a Coulomb attraction.[18] The effects of carrier screening, phase-space filling, and band-gap renormalization are neglected, except for one case discussed later, where they are included phenomenologically.

When calculating an individual e-h-pair response, however, two-body processes such as carrier-carrier and carrier-phonon scattering become important soon after excitation. Three constants, Γ, γ, and Λ, are used to simulate the various relaxation effects. For instance, the rate of intraband scattering in which the electron or hole inelastically scatters to different nonresonant states within the same band is given by Γ. The dephasing of the dipoles (the nondiagonal elements of the density matrix) is characterized by the dipole decay rate γ. Finally, Λ takes into account that in the nearly full valence band the optically created empty states are filled incoherently from other states.

Using these simplifying assumptions the DTS are calculated and compared below to our data for all three cases.

A. Case (i)

Here the pump is tuned well above the band edge, bound states are neglected, and a pump field amplitude, $\mathcal{E}_L$, which is small in comparison to that of a π pulse, is assumed. Under these conditions the probe-transmission changes around the pump frequency Ω_L are given as [see Eq. (14) of preceding paper]

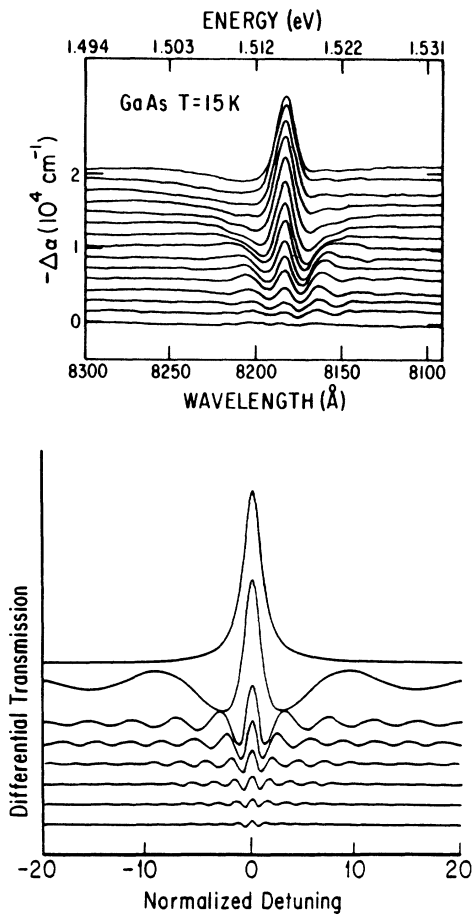

FIG. 7. (a) Measured differential transmission around the exciton resonance in a 0.5-μm-thick MBE-grown layer of GaAs at 15 K, for pumping above band. The pump pulse is centered around 620 nm with 60-fs duration. The spectra are taken 100 fs apart; (b) differential transmission spectra calculated in the vicinity of the exciton resonance ω_x. The pump is high into the band with $\Omega_L \gg \omega_x$. The curves are in 50-fs intervals with the bottom trace for -350-fs and the top trace for 0-fs time delays.

$$\delta T(\omega) = T' \,\mathrm{Re}\left[\int_0^\infty dt\, e^{i(\omega-\Omega_L)t} e^{-2\gamma t} \int_0^\infty dt' e^{-\Gamma t'} \mathcal{E}_L(t_p - t') \mathcal{E}_L^*(t_p - t' - t)\right] + T' \,\mathrm{Re}\left[\int_0^\infty dt\, e^{i(\omega-\Omega_L)t} e^{-\Gamma t} \int_0^t dt' e^{-(2\gamma-\Gamma)t'} \mathcal{E}_L(t + t_p - t') \mathcal{E}_L^*(t_p - t')\right], \quad (1)$$

where T' is a combination of constants. The delay time, t_p, between the pump and probe pulses is negative for situations where the probe pulse is ahead of the pump pulse.

The calculated results of Eq. (1) are plotted in Fig. 2(b) for several values of t_p. A few comments are in order here. First, the plots shown in Fig. 2(b) [as well as those in Fig. 5(b)] were calculated using a pump pulse with an envelope shape $E_p \propto e^{-\sigma|t|}$, where σ describes the temporal pulse width. This unphysical shape simplified analytical calculations, and differed very little from results obtained using a more realistic sech pulse shape.[17] Similarly, a temporal δ-function probe pulse was used in the calculations; however, as is shown in the Appendix of Ref. 19, the results are essentially unchanged for longer probe pulses.

The frequency of the oscillations in Fig. 2(b) is determined by the time delay between pump and probe. Increasing the temporal overlap between the pulses causes a decrease in the number of oscillations and an increase in the amplitude of these oscillations with respect to the central peak. These results are in qualitative agreement with the experimental case (i). A plot of the calculated frequency of oscillations (inverse of the fringe spacing) versus t_p is the straight line shown in Fig. 4. The experimental data points are represented by data bars, and lie on or close to this line.

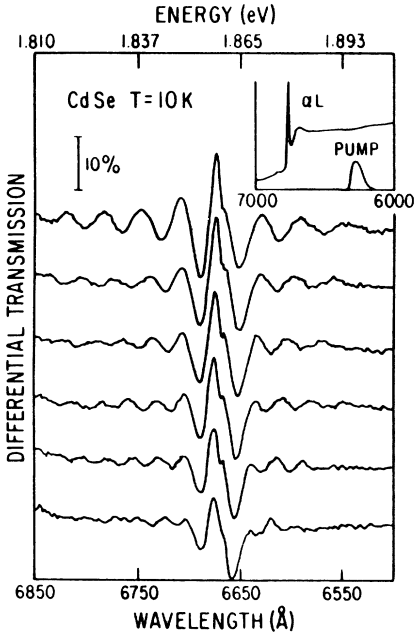

FIG. 8. Measured differential transmission spectra around the exciton resonance of a 0.5-μm-thick CdSe platelet at 10 K for pumping into the band. The pump pulse is centered around 620 nm, it has a 150-fs FWHM, and a peak intensity of 10^9 W/cm^2. The different spectra are 50 fs apart.

An analysis of the relative importance of the different damping processes shows that the shape of the oscillatory structures is rather insensitive to the value of the dipole damping rate γ. Even for large values of γ, the only effect of increasing γ is the overall decrease of the spectra. On the other hand, the calculations show that the DTS in this region is quite sensitive to the population decay rate, Γ, which simulates the intraband scattering of the laser-excited carriers. Increasing Γ decreases the amplitude of the oscillations with respect to the central peak until, for large Γ only a broadened peak, the spectral hole, is left.

B. Case (ii)

For case (ii), when the pumping takes place below the band but the δT in the spectral region around the exciton is analyzed, the exciton is modeled as a single homogeneously broadened transition and contributions from the band states are neglected. If the pump detuning from the exciton, $\Omega_L-\omega_x$, largely exceeds both the exciton linewidth γ_x and the spectral width of the pump, the differential transmission as a function probe detuning, $\Delta=\omega-\omega_x$, is

$$\delta T(\omega)\cong -C_0\frac{1}{\omega_x-\Omega_L}\times \mathrm{Im}\left[\frac{1}{\gamma_x-i\Delta}\int_0^\infty dt\,|\,\mathscr{E}_L(t+t_p)\,|^2 e^{i\Delta t-\gamma_x t}\right], \tag{2}$$

where C_0 is a combination of constants [see Eq. (18) of preceding paper]. This differential transmission is plotted in Fig. 5(b) for various t_p. Oscillations in the differential transmission spectra are now expected around the exciton frequency and should have the features displayed in Fig. 5(b). The structures should not be symmetric as in the case of the resonant interband transitions, but rather asymmetric because the pump laser is detuned from the exciton resonance. As the delay time approaches zero, the oscillations should change gradually into the dispersive shape characteristic for the optical Stark shift of the exciton resonance. In fact, in Eq. (2) oscillations occur if the integrand has a peak between the limits of the integral, that is, if the time delays are negative only. These qualitative features are observed in the experimental Figs. 5(a) and 6. Hence, the oscillatory structures can be viewed as the early stages of the optical Stark effect in short-pulse pump-probe spectroscopy, and Eq. (2) can be regarded as generalization of the Stark-shift result obtained in the adiabatic limit.[14] Note that Eq. (2) also expresses that the amplitude of oscillations falls off with the detuning of the pump from the exciton, whereas the shape of the oscillations is detuning independent.

C. Case (iii)

When the pump is far above the band and there is no spectral overlap between pump and probe, many-body Coulomb effects cannot be neglected, because they represent the only mechanism by which the pump-generated electrons and holed modify the exciton resonance. The major consequence of these many-body Coulomb effects between the exciton and the excited electrons and holes inside the band is a bleaching of the exciton resonance.[13] The pump-induced exciton bleaching is modeled as a time-dependent dipole damping, where the damping rate increases with increasing pump-pulse intensity. In other words, γ is replaced with $\gamma(t)$ in the Bloch equation for the exciton state. This simple model yields

$$\delta T(\omega)\propto \begin{cases} \mathrm{Re}\left[\dfrac{1}{\gamma-i\Delta}e^{(-i\Delta+\gamma_0)t_p}\right] & \text{for } t_p<0\,, \\ \mathrm{Re}\left[\dfrac{1}{\gamma-i\Delta}\right] & \text{for } t_p>0\,, \end{cases} \tag{3}$$

where $\gamma(t)=\gamma_0+\delta\gamma(t)$.

A numerical evolution of Eq. (3) is shown in Fig. 7(b) and is in good qualitative agreement with the experimental observations of Fig. 7(a) and 8.

V. DISCUSSION

There are some differences in the physical origins of the oscillations which occur in the band and those centered around the exciton. In the latter case the pump interacts not only with the probe-induced polarization when there is temporal overlap of pump and probe, but also with the coherent polarization remaining in the sample after complete transmission of the probe through the sample. In the former case there is interaction between the pump and the probe-induced polarization only when the two pulses are overlapped in the sample.

The reason for the difference lies in the fact that the free induction decay (FID) of the exciton state is much longer than the probe-pulse duration, while the effective FID of the composite system of unbound *e-h* pairs is not. Brito Cruz *et al.*[15] discuss this point explicitly when analyzing oscillations in the transmission spectra of organic dyes. They used a perturbative approach which separates into two terms the interactions which occur in the sample when the exit of the probe pulse precedes the arrival of the pump pulse, and those that occur when the two pulses are overlapped in the sample. On the other hand, the theoretical approach applied in this paper[17–19] to cases (i) and (ii) incorporates both these terms into one. It is the energy integration over the effective density-of-states term, discussed at the beginning of the preceding section, that causes the FID in the band and at the exciton frequency to have different importance. In fact, while a major contribution to the oscillations around the exciton may be considered a result of a perturbation of its FID,[13] the oscillations around the pump, when it is tuned above the band, must be viewed primarily as scattering of the pump from a grating produced by the probe and a leading part of the pump which has some temporal overlap with the probe.

Regardless of the details of an excitation, however, it can be shown quite generally[19] that oscillations in differential transmission spectra are expected as long as the pump field produces any substantial change in the total transmitted probe field. In this paper we reported three such cases of oscillations in the differential transmission spectra detected using femtosecond pump-probe spectroscopy. For case (i) the change in probe transmission results in oscillations at the pump position, which finally evolve into the spectral hole when the time delay approaches zero. In case (ii) it is the change in the probe transmission due to the early stages of the Stark shift of the exciton, which leads to the oscillations in the vicinity of exciton. And, finally, for case (iii) the pump bleaches the exciton by many-body Coulomb effects. The oscillations in δT in this case evolve into the exciton line shape, which is characteristic for the bleached exciton. There is good agreement between theory and experiment for all three cases.

ACKNOWLEDGMENTS

The authors would like to acknowledge support from the National Science Foundation (Grant No. 8610170), JSOP, the North Atlantic Treaty Organization Travel Grant No. 86/0749), ONR/SDIO) (Grant No. N00014-86-K-0719), DARPA/RADC (Grant No. F30602-87-C-0009), DRET (France), the John von Neumann computer Center (Princeton, NJ) for the CPU time, and the Optical Circuitry Cooperative of the University of Arizona. We would also like to thank V. Williams and W. Hahn for help in the laboratory. We gratefully acknowledge fruitful discussions with C. Benoit à la Guillaume. M. Joffre and D. Hulin are also with the Groupe de Physique des Solides de l'Ecole Normale Supérieure.

[1]C. V. Shank, R. L. Fork, R. F. Leheny, and J. Shah, Phys. Rev. Lett. **42**, 112 (1979).

[2]D. von der Linde and R. Lambrich, Phys. Rev. Lett. **42**, 1090 (1979).

[3]R. F. Leheny, J. Shah, R. L. Fork, C. V. Shank, and A. Migus, Solid State Commun. **31**, 809 (1979).

[4]A. L. Smirl, T. F. Boggess, B. S. Wherrett, G. P. Perryman, and A. Miller, Phys. Rev. Lett. **49**, 933 (1982).

[5]J. L. Oudar, A. Migus, D. Hulin, G. Grillon, J. Etchepare, and A. Antonetti, Phys. Rev. Lett. **53**, 384 (1984).

[6]J. L. Oudar, D. Hulin, A. Migus, A. Antonetti, and F. Alexandre, Phys. Rev. Lett. **55**, 2074 (1985).

[7]W. H. Knox, C. Hirlimann, D. A. B. Miller, J. Shah, D. S. Chemla, and C. V. Shank, Phys. Rev. Lett. **56**, 1191 (1986).

[8]L. Schultheis, M. D. Sturge, and J. Hegarty, Appl. Phys. Lett. **47**, 995 (1985).

[9]L. Schultheis, J. Kuhl, A. Honold, and C. W. Tu, Phys. Rev. Lett. **57**, 1797 (1986).

[10]A. Mysyrowicz, D. Hulin, A. Antonetti, A. Migus, W. T. Masselink, and H. Morkoç, Phys. Rev. Lett. **56**, 2748 (1986).

[11]A. Von Lehmen, D. S. Chemla, J. E. Zucker, and J. P. Heritage, Opt. Lett. **11**, 609 (1986).

[12]B. Bluegel, N. Peyghambarian, M. Lindberg, S. W. Koch, M. Joffre, D. Hulin, A. Migus, and A. Antonetti, Phys. Rev. Lett. **59**, 2588 (1987).

[13]M. Joffre, D. Hulin, A. Migus, A. Antonetti, C. Benoit à la Guillaume, N. Peyghambarian, M. Lindberg, and S. W. Koch, Opt. Lett. **13**, 276 (1988).

[14]S. Schmidtt-Rink and D. S. Chemla, Phys. Rev. Lett. **57**, 2752 (1986).

[15]C. H. Brito Cruz, J. P. Gordon, P. C. Becker, R. L. Fork, and C. V. Shank, IEEE J. Quantum Electron **QE-24**, 261 (1988).

[16]In order to obtain the zero time delay, it is customary to perform a sum frequency generation on a nonlinear crystal mounted near the sample. The results of such a scheme gave a zero time delay which had to be shifted by + 200 fs in Figs. 2(a), 3, and 5(a). Such a shift seems to be not unreasonable considering that the determination of the zero time delay by nonlinear frequency mixing involves the replacement of the nonlinear crystal by the sample under investigation. Slightly different path lengths for the two pulses on the sample may easily result in uncertainty of a couple of hundred femtoseconds in the absolute zero time delay. As discussed in the text, the oscillations gives an accurate method for determining the absolute time delay.

[17]M. Lindberg and S. W. Koch, J. Opt. Soc. Am. B **5**, 139 (1988).

[18]M. Lindberg and S. W. Koch, Phys. Rev. B **38**, 3342 (1988).

[19]M. Lindberg and S. W. Koch, preceding paper, Phys. Rev. B **38**, 7607 (1988).